Journal of Thermal Analysis, Vol. 46 (1996) 1271-1282

NON-ISOTHERMAL KINETICS OF CrO_3 DECOMPOSITION PATHWAYS IN AIR

Nasr E. Fouad

Chemistry Department, Faculty of Science, Minia University, El-Minia 61519, Egypt

(Received April 14, 1995)

Abstract

The course of the non-isothermal decomposition of CrO_3 in air was explored kinetically, by using a number of widely accepted methods. The credibility of the values obtained from a given kinetic parameter (the reaction order, the activation energy and the frequency factor) was justified on the grounds of (i) a multiple correlation coefficient, and (ii) the merits and demerits of the method adopted. The results obtained may help towards a characterization of the non-isothermal conditions under which the encountered decomposition events and products could be resolved. The study was motivated by the results of previous physicochemical characterization studies [1, 2], in which catalytically important intermediates $CrO_x(3<x<6)$ were structurally identified.

Keywords: CrO_3, kinetics

Introduction

The results of studies conducted in this laboratory [1, 2] are in line with those of other studies [3–6] in showing that the thermal decomposition of CrO_3 into Cr_2O_3 at 523–753 K in air involves the formation of three detectable intermediate CrO_x phases. These are $CrO_{2.66}$, at 523–593 K, $CrO_{2.5}$, at 593–623 K, and $CrO_{2.25}$, at 658–703 K. X-ray diffractometry revealed [2] the following compositions: Cr_3O_8, Cr_2O_5 and Cr_4O_9, respectively. Infrared spectroscopy demonstrated [1, 2] that the genesis of these intermediates involves the establishment of Cr–O–Cr bridge bondings. Thus, a polymerization process has been seen [1–4] to follow heat-induced oxygen release [3, 4]. However thermal analyses have shown that the formation pathways of the intermediates overlap considerably [1, 2].

The XRD-verified compositions for the intermediates CrO_x are indicative of composite material bulks containing mixed valency (in the range from Cr^{6+} to Cr^{3+}) chromium-oxygen species [2, 7]. Such materials are anticipated to exhibit potential surface catalysis in redox processes [8, 9]. The redox activity of

0368–4466/96/ $ 5.00

John Wiley & Sons, Limited
Chichester

CrO_x based catalysts towards H_2O_2 [10] and isopropanol [11] decomposition reactions has been found to be closely related to the exposure on the surface of intimately coupled Cr ions in different oxidation states. Such an intimate coupling has been suggested [8, 12, 13] to facilitate *d–d* electron exchange interactions and, consequently, the electron mobility across the surface. Systematic magnetic and optical spectroscopic measurements [8] allowed monitoring of the formation of such mobile-electron phases (denoted Zener phases [12]) on chromia. It has even been claimed [8] that the availability of these phases creates the ideal environment in which not only the redox activity, but also the polymerization activity is optimized.

The present paper reports and discusses results of a non-isothermal kinetic study of the pathways of CrO_3 decomposition in air, obtained via widely accepted methods and models [14]. The study had the basic aim of characterizing non-isothermal conditions for production of the intermediate CrO_x in separate bulk phases. The non-isothermal approach was adopted, despite some kinetic reservations [14], in view of the fact that the isothermal synthesis of solids is often attained by effective sintering. In work with catalytic solids, textural consequences of sintering, such as the loss of surface accessibility [15], are undesirable.

Experimental

Chromium trioxide

Chromium trioxide, CrO_3, was a 99.9% pure product of Riedel-de Hean AG (Hannover/Germany). Prior to application, it was subjected to drying at 383 K in air and maintained dry over P_2O_5.

Thermal analysis

Thermogravimetry (TG), differential thermogravimetry (DTG) and differential thermal analysis (DTA) measurements were made in a dynamic atmosphere of air (20 ml min^{-1}) with a model 30-H Shimadzu thermal analyzer (Japan). The temperature was increased linearly at different heating rates (β)=2, 5, 10, 20 and 50 K min^{-1}. Comparably small amounts of CrO_3 (10–15 mg) were used for the TG measurements; α–Al_2O_3 was the thermally inert reference for DTA.

Kinetic methods and data processing

Table 1 lists the kinetic methods and equations [14, 16–20] that were implemented in analysing the data measured by the thermoanalytical technique. The analysis was designed with the aim of calculation of the activation energy (ΔE), the frequency factor (A) and the order (n) for the decomposition reactions of

Table 1 Non-isothermal methods and equations used for the kinetic analysis

Method	Technique	Equation	Ref.
Kissinger	DTA	$\ln(\beta/T_p^2) = -(\Delta E/R)/T_p + \ln(AR/\Delta E)$	[14, 16]
Coats-Redfern	TG	$\log[1-(1-\alpha)^{1-n}/T^2(1-n)] = \log(AR/\beta\Delta E) - (\Delta E/2.3R)/T; \quad n \neq 1$	[17]
		$\log[-\log(1-\alpha)/T^2] = \log(AR/\beta\Delta E) - (\Delta E/2.3R)/T; \quad n = 1$	
Freeman-Carroll	TG	$\Delta\log(dw/dT)/\Delta\log W_r = -(\Delta E/2.3R)\Delta T^{-1}/\Delta\log W_r + n$	[18]
Jerez	TG	$n = Y/(1-QX)$	[19]
		$\Delta E = RQY/(1-QX)$, where $Q = [(d\alpha/dT)/(1-\alpha)]_{\alpha=\max}$	
Ozawa	DTG	$\ln(\beta/T_m^2) = -(\Delta E/R)T_m + \ln(R/\Theta\Delta E)$	[20]

β, heating rate (K min^{-1}); R, gas constant (=8.3 J K^{-1} mol^{-1}); T_p, DTA peak temp. (K); α, fraction of reaction completed; $W_t = (W_c - W_t)$ W_t and W_c being respectively the weight losses at time t and at reaction completion; Y, mean value of left-hand side values of Freeman–Carroll equation; X, mean value of right-hand side values of Freeman–Carroll equation; Θ, reduced time; and T_m, DTG peak temp. (K).

CrO_3 encountered. A computer program was applied for the data-processing, whereby the results best fitting the equations were monitored via the multiple correlation coefficient (R^2): the closer its value to unity, the better the fitting.

The activation entropy (ΔS) was also calculated by using the following equation [21, 22] where k is the Boltzmann constant and h is the Planck constant.

$$\Delta S = R\ln(Ah/kT_p)$$

Results and discussion

Decomposition course and products

Figure 1 compares thermal analysis results (obtained at 2 K min^{-1}) on CrO_3. Similarly as in earlier investigations [1, 2], the present results demonstrate the occurrence of four thermal events (denoted I–IV) in the course of CrO_3 decom-

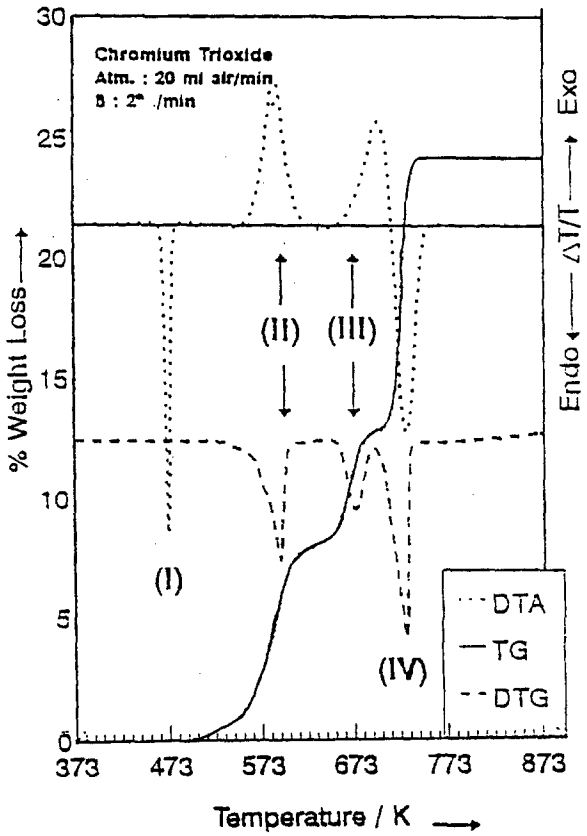

Fig. 1 Thermoanalytical curves for CrO_3 in air

position. These events were previously [2] characterized physicochemically by means of X-ray diffractometry, and UV/Vis diffuse reflectance and infrared spectroscopy. The results are reviewed in Table 2.

Table 2 shows that thermal event II is composite and involves the decomposition of CrO_3 into $CrO_{2.66}(=Cr_3O_8 \cong CrO_3 \cdot Cr_2O_5$ or $2CrO_3 \cdot CrO_2)$, and the subsequent conversion of the latter into $CrO_{2.5}(=Cr_2O_5$ or $CrO_3 \cdot CrO_2)$. Table 2 also shows that $CrO_{2.25}$ $(=Cr_4O_9)$ should be the sole product of event III (at 673–723 K; T_{max}=698 K). Nevertheless, the analysis of products of CrO_3 at 673 and 723 K for 3 h failed to reveal the existence of crystalline Cr_4O_9 [2]. The sole crystalline phase detected in this temperature range was α-Cr_2O_3. This was tentatively attributed to kinetic reasons [2].

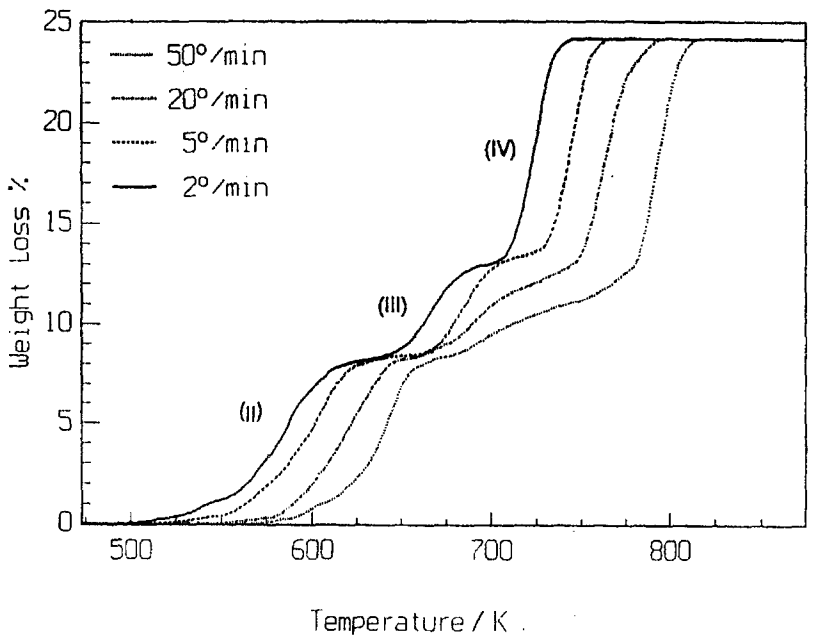

Fig. 2 Thermogravimetry of CrO_3 as a function of the heating rate

Influence of heating rate

TG curves recorded as a function of the heating rate (β=2–50 K min^{-1}) are compared in Fig. 2. It is obvious that the temperatures at which events II–IV are maximized suffer high-value shifts on increase of the heating rate. Similar behaviour was observed for the DTA peak temperatures; the results are summarized in Table 3.

Moreover, Fig. 2 shows that the rate of change ($\Delta W/\Delta T$) of event II is enhanced, whereas that of event III is diminished, as the heating rate is increased.

Table 2 Characteristics of thermal events and products encountered (at 2 K min^{-1}) throughout the decomposition course of CrO_3 in air [2]

Event	T_{max}/K	$\Delta T/T$	$\Delta W/T$	Change undertaken	Product
I	473	endo	invariant	melting	CrO_3
II	588	exo	variant	$CrO_3 \rightarrow CrO_{2.66} \rightarrow CrO_{2.5}$	Cr_3O_8 and Cr_2O_5
III	698	exo	variant	$CrO_{2.5} \rightarrow CrO_{2.25}$	Cr_4O_9
IV	728	endo	variant	$CrO_{2.25} \rightarrow CrO_{1.5}$	Cr_2O_3

Table 3 DTA peak temperatures (K) as a function of the heating rate

Event	2 K min^{-1}	5 K min^{-1}	20 K min^{-1}	50 K min^{-1}
I	473	481	491	495
II	588	600	633	653
III	698	713	728	735
IV	728	750	783	808

In contrast, the rate of event IV is rather indifferent to changes of the heating rate. It is worth noting, however, that the enhancement of event II, which is confined to the final part of it, is evident only upon increase of the heating rate from 20 to 50 deg min^{-1}. In contrast, the retardation of event III occurs rather gradually on increase of the heating rate.

Credibility of kinetic methods and parameters

The activation energy (ΔE) was calculated for the various events (I–IV) by using five different methods, as indicated in Table 4. In contrast, the frequency factor (ln A) was obtained from the data given in Table 2 by using Kissinger's method. The correlation devised by Kissinger [14, 16] facilitates the obtaining of both ΔE and ln A for a given event from the slope and intercept of linear plots of $\ln(\beta/T_p^2)$ *vs.* $1/T_p$ (Fig. 3). Kissinger's method is distinct in adopting the DTA

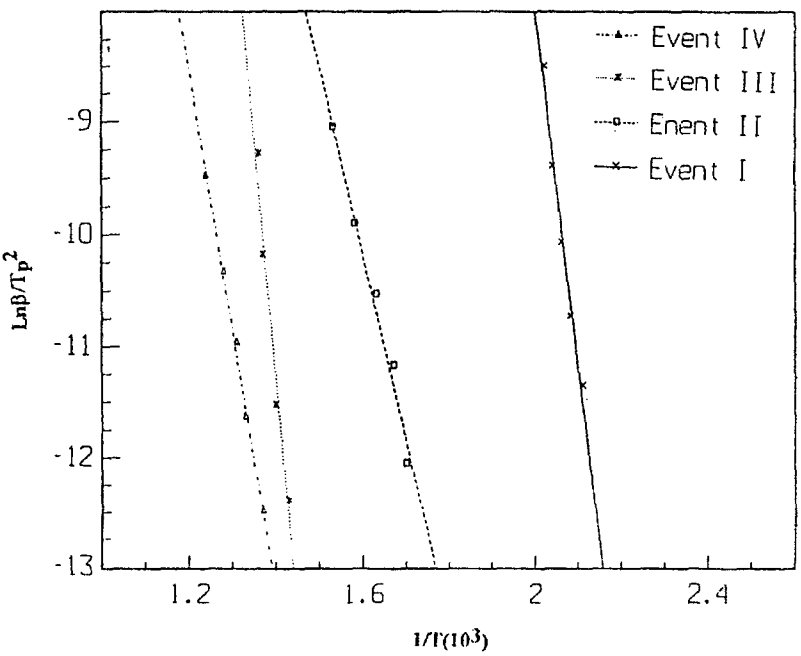

Fig. 3 The Kissinger's plot for the events monitored in the DTA curves of CrO_3

Table 4 Non-isothermal kinetic parameters derived for the thermal events indicated

Method	Kissinger			Ozawa		Coats-Redfern			Freeman-Carroll			Jerez		Entropy
Data	DTA			DTG		TG			TG			TG		DTA
event	ΔE	$\ln A$	R^2	ΔE	R^2	n	ΔE	R^2	n	ΔE	R^2	n	ΔE	ΔS
I	287	16.5	0.993	–	–	–	–	–	–	–	–	–	–	–156.7
II	140	11.4	0.982	180	0.970	1	134	0.996	0.5	158	0.995	0.52	102	–125.8
						2/3	121	0.997						
						1/2	104	0.996						
						0	98	0.994						
III	341	15.2	0.965	260	0.820	1	371	0.972	0.0	284	0.750	0.59	317	–153.0
						2/3	372	0.977						
						1/2	330	0.968						
						0	290	0.952						
IV	196	12.0	0.996	214	0.942	1	672	0.974	0.0	501	0.992	0.30	485	–112.0
						2/3	585	0.991						
						1/2	585	0.992						
						0	518	0.997						

ΔE, activation energy (kJ mol^{-1}); $\ln A$, frequency factor; n, reaction order; ΔS, activation entropy (J mol^{-1} K^{-1}); and R^2, correlation coefficient.

results. Thus, it is superior to the other methods for its ability to handle not only the mass-variant, but also the mass-invariant (e.g. event I) processes. However, it does not consider the actual reaction order (n) [14]. This disadvantage may give some credit to the methods of Coats-Redfern and Freeman-Carroll (Tables 2 and 4), which allow for the determination of 'n', but with the adoption of different approaches to the TG results. The Coats-Redfern method [17] operates a trial-and-error technique, whereby the 'n' value to be considered is the value that achieves the best linearity of the variables related by the equations of the method (Table 1). A sample result, considering event II, is presented in Fig. 4. On the other hand, the Freeman-Carroll method [18] adopts a straightforward approach, whereby the order is obtained directly from the relationship devised (Table 1). Therefore, it is considered [14] to be more convenient and less time consuming than the Coats-Redfern method. Nevertheless, it has been criticized for being less accurate [14]. In response to the criticism, Jerez [19] has modified the Freeman-Carroll approach, applying statistical analysis to the data. The 'n' values thereby obtained are thought [14] to be more accurate than the Freeman-Carroll values.

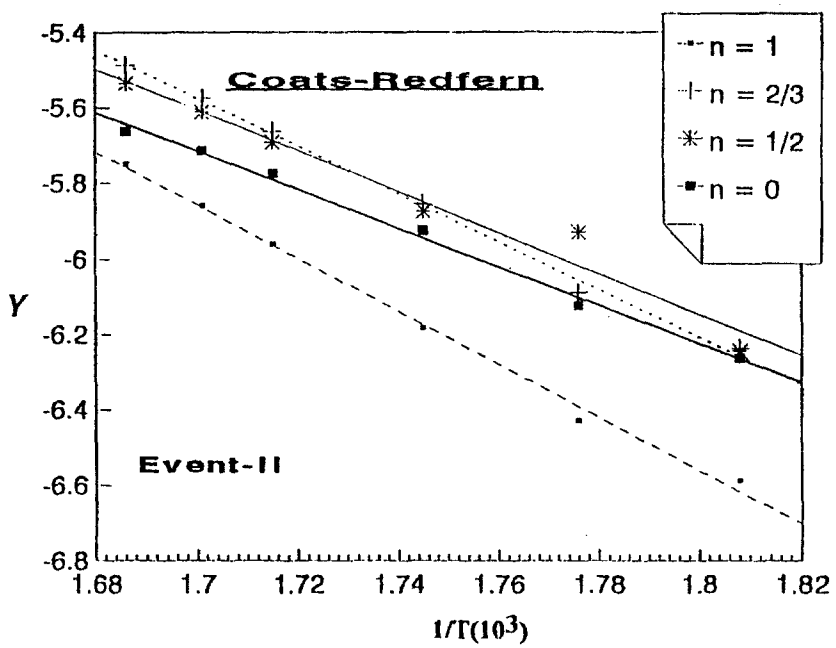

Fig. 4 Coats-Redfern's plot for event II assuming the reaction order values indicated; $Y=\log[-\log(1-\alpha)/T^2]$ for $n=1$, and $Y=\log[1-(1-\alpha)^{1-n}/T^2(1-n)]$ for other n values

In the present study, the credibility of the values of a given kinetic parameter (either ΔE or n) calculated by using different methods is justified on the following grounds: (i) the multiple correlation coefficient (R^2) value, and (ii) the merits and demerits of the method adopted, as reviewed above. On these grounds,

the credible values of ΔE and n for each of the events (I–IV) encountered throughout the course of CrO_3 decomposition are those underlined in Table 4. These values will be considered exclusively in the discussion of the kinetics of the events below. It is worth noting, however, that the credibility test shows clearly that the method of Coats-Redfern and its version as modified by Jerez are superior to the other methods in determining accurate values for ΔE and n for mass-variant processes of CrO_3 decomposition.

Kinetics of decomposition events of CrO_3

Event I: CrO_3 (solid)→CrO_3(melt)

For the mass-invariant melting process involved, the values obtained for ΔE (287 kJ mol^{-1}), ΔS (−156.7 J mol^{-1} K^{-1}) and ln A (16.5) are relatively high in magnitude (Table 4). Such a process occurs without nucleation, and consists of two basic steps: (i) a phase boundary process; and/or (ii) transport processes to or from the reacting interface [14]. The high entropy and frequency factor values are quite consistent with the disordering expected to follow the melting. As concerns the activation energy, the high value cannot be credited, since it was obtained by using a single method (Kissinger's). Nevertheless, it might account for a slow process due to the chain-structure assumed by solid-phase CrO_3 [1].

Event II: CrO_3→Cr_3O_8→Cr_2O_5

The kinetic analysis allocates a fractional reaction order to the event in the range n=0.52–0.66, and in the ΔE range 102–121 kJ mol^{-1}. The ΔS and ln A values allocated (Table 4) are lower than the values determined for the preceding event I. These latter changes go well with the re-ordering expected to follow the solidification and formation of product crystallites [2]. In contrast with homogeneous-like kinetics, fractional or even negative reaction orders are observed in the solid state [14]. It has been shown [23, 24] that the reaction order 'n' in the solid state is by no means a universal constant. It has been defined [23, 24] that the reaction order 'n' in the solid state is by no means a universal constant. It has been defined [23, 24] as being just a useful monitor of the change in the kinetics of processes conducted under different conditions [14]. The order value (ca. 2/3) accounts for a phase boundary-controlled process [14], which is in accordance with the corresponding low ΔE values. It seems that the crystallites formed [2] do not impose any significant restriction on the product accommodation in the lattice.

It is to be noted, however, that the shape of the occurrence of the event in the TG curve (Fig. 2) is asymmetrically influenced by change of the rate of heating (from 20 to 50 K min^{-1}). We believe that this behaviour is consistent with the composite nature of the event. The rate of change ($\Delta W/\Delta T$) of the initial step

$CrO_3 \rightarrow Cr_3O_8$ appears to be largely unaffected by the increase of β, whereas that of the following step $Cr_3O_8 \rightarrow Cr_2O_5$ increases. This may imply that the exothermic nature revealed for the event (Fig. 1) is actually a net result of a compensation involving largely overlapping exo- and endothermic reactions. Thus, a thermal resolution of the two steps might be possible when heating is carried out at <2 K min^{-1}.

Event III: $Cr_2O_5 \rightarrow Cr_4O_9$

The ΔE value (317–372 kJ mol^{-1}) obtained for the present event is considerably higher than that of the preceding event II, though the reaction order values (ca. 2/3) are quite comparable (Table 4). In contrast, the ΔS and ln A values are higher for the present event than for the preceding one (Table 4). The similarity between the order values implies that event III also involves a phase boundary-controlled process. The increases in the values of both the entropy and the frequency factor account for a disordering (or a less-ordering) mechanism, which can be correlated with the failure to detect a crystalline Cr_4O_9 phase in the course of CrO_3 decomposition at 673–723 K [2]. In view of these results, the considerable increase in the activation energy may be correlated with the marked decrease in the rate of change ($\Delta W/\Delta T$) of the event as β is increased (Fig. 2). The exothermic nature of the event (Fig. 1) may justify the correlation proposed.

Event IV: $Cr_4O_9 \rightarrow Cr_2O_3$

Previous XRD analysis identified the product of the event as being α-Cr_2O_3. The α-structure of chromia hexagonal close packing, is the most stable structural modification for chromium oxides [25]. Thus, the change observed in the reaction kinetics, as manifested by the changes in the reaction order (from $\approx$2/3 to $\leq$1/3) and activation energy (from 317–372 to 485–518 kJ mol^{-1}) values, is explicable. In the wake of the formation of a close-packed structure such as α-Cr_2O_3, the reaction undertaken would be predominantly diffusion-controlled. This type of reactions demands significantly high activation energies [14]. In full compliance with the expected ordering mechanism, both ΔS and ln A assume the relatively lowest values (Table 4) amongst those for the four events encountered.

References

1 M. I. Zaki and R. B. Fahim, J. Thermal Anal., 31 (1986) 825.
2 N. E. Fouad, Bull. Fac. Sci. Assiut Univ., Assiut, Egypt, 22, 1-B (1993) 55.
3 T. V. Rode, Oxygen Compounds of Chromium Catalysts, Izd. Akad, Nauk SSSR, Moscow 1962, pp. 72–95.

4 T. V. Rode, in J. P. Redfern (Ed), Thermal Analysis, Macmillan, London 1965, pp. 122–123.
5 H. Park, Bull. Chem. Soc. Japan, 45 (1972) 2749.
6 H. Park, ibid, 45 (1972) 2753.
7 A. F. Wells, Structural Inorganic Chemistry, 3rd edn., Clarendon Press, London 1978, p. 947.
8 A. Ellison, J. O. V. Oubridge and K. S. W. Sing, Trans, Faraday Soc., 66 (1970) 1004; A. Ellison and K. S. W. Sing, J. Chem. Soc., Faraday Trans. I, 74 (1978) 2807.
9 M. I. Zaki, N. E. Fouad, J. Leyrer and H. Knözinger, Appl. Catal., 21 (1986) 359.
10 R. B. Fahim, M. I. Zaki and R. M. Gabr, Surf. Technol., 12 (1982) 317.
11 R. B. Fahim, M. I. Zaki and R. M. Gabr, Appl. Catal., 4 (1982) 189.
12 C. Zener, Phys. Rev., 82 (1951) 403.
13 G.-M. Schwab and S. B. Kanungo, Z. Phys. Chem., NF, 107 (1977) 109.
14 J. Šesták, V. Satava and W. W. Wendlandet, Thermochim. Acta, 7 (1973) 333.
15 K. S. W. Sing and S. J. Gregg, Adsorption, Surface Area and Porosity, Academic press, London 1967, p. 3 and p. 309.
16 H. E. Kissinger, J. Anal. Chem., 29 (1959) 1702.
17 A. W. Coats and J. P. Redfern, Nature, 201 (1969) 2060.
18 E. S. Freeman and B. Carroll, J. Phys. Chem. 62 (1958) 394.
19 A. Jerez, J. Thermal Anal., 26 (1983) 315.
20 (a) T. Ozawa, J. Thermal Anal., 2 (1970) 301; and (b) J. Thermal Anal., 7 (1975) 601.
21 Z. Lu and L. Yang, Thermochim. Acta, 188 (1991) 135.
22 S. M. K. Nair and C. James, Thermochim. Acta, 96 (1985) 27.
23 J. Šesták, in H. G. Wiedemann (Ed.), Thermal Analysis, Vol. 2, Birkhäuser Verlag, Basel 1972, p. 3.
24 G. W. Brindley, J. H. Sharp and B. N. N. Achar, in J. P. Redfern (Ed.), Thermal Analysis, Mcmillan, London 1965, p. 180.
25 In Ref. [7], p. 450.